A COMPREHENSIVE PHOTOMETRIC INVESTIGATION OF 185 EUNIKE

Frederick Pilcher
4438 Organ Mesa Loop
Las Cruces, NM 88011 USA
pilcher@ic.edu

Raoul Behrend, Laurent Bernasconi
Observatoire de Geneve
Geneva, SWITZERLAND

Lorenzo Franco
Balzaretto Observatory (A81)
Rome, ITALY

Kevin Hills
Riverland Dingo Observatory (RDO)
Moorook, 5343, South Australia
AUSTRALIA

Axel Martin
Turtle Star Observatory (TSO)
Friedhofstr. 15
45478 Muelheim-Ruhr
GERMANY

John C. Ruthroff
Shadowbox Observatory
12745 Crescent Drive
Carmel, IN 46032 USA

(Received: 6 July)

We have reevaluated our previous photometric data sets of 185 Eunike for oppositions in the years 2010, 2011, and 2012, respectively, and have obtained new observations in 2014 Jan. - May. For each of these four years we draw period spectra which show deep minima only near 21.8 hours and the double period near 43.6 hours, and plot lightcurves phased to near 21.8 and 43.6 hours, respectively. For observation sets in each of the four years we find the available parts of the lightcurves phased to 43.6 hours and separated by 1/2 cycle to be identical within errors of observations, and conclude that the double period is ruled out. For the new observations in the year 2014 we find best fit to a lightcurve phased to 21.812 ± 0.001 hours with amplitude 0.08 ± 0.01 magnitudes. The absolute magnitude and the opposition parameter are H = 7.45 ± 0.01, G = 0.11 ± 0.02. The V-R color index was determined to be 0.36 ± 0.03. Both the color index and G value are compatible with a low albedo asteroid. The diameter is estimated to be D = 175 ± 33 km. The lightcurve inversion analysis shows a preliminary sidereal period/pole solution at Ps = 21.80634 ± 0.00012 h and (λ = 136°, β = 4°), (λ = 314°, β = -18°), with an error estimation of ± 30 degrees.

Debehogne et al. (1978) published a period of 10.83 hours based on rather sparse data. No further photometric observations were made for many years. In 2005 February – March two lightcurves were acquired by Behrend (2005) with no period estimation. In 2010 April - May dense data sets were by Ruthroff (2010), who suggested a period of 11.20 hours, and by Behrend (2010), who suggested a period of 21.807 hours. Ruthroff (2011) reevaluated

his 2010 data and found them consistent also with 14.56 hours. Pilcher and Ruthroff (2012) examined these data again and found them consistent with a period of 21.80 hours. Another dense data set was obtained in 2011 June - August by Pilcher and Ruthroff (2012) who published a period of 21.797 hours. Still another data set was obtained in 2012 Nov. - Dec. by Hills (2013) who obtained a period of 21.777 hours. All of these investigations were with differential photometry only without comparison with catalog magnitudes. An examination of the lightcurve by Debehogne et al. (1978) suggests that their data are also compatible with twice their 10.83 hour period. It is noteworthy that the near 21.8 hour period found at all three oppositions, 2010, 2011, and 2012, features a somewhat wavy lightcurve with one maximum and minimum per cycle of approximately 21.8 hours. This suggests that the lightcurve form is dominated by hemispheric albedo variegation rather than the usual elongated shape.

In this paper the authors of all three of the data sets from the years 2010, 2011, and 2012, respectively, reevaluate their data. Additional observations were made 2014 Jan. 16 - May 4 by authors Pilcher, Franco, Hills, and Ruthroff. These new data used the Comparison Star Selector of *MPO Canopus* software and solar colored stars, which in addition to low noise lightcurves allowed a reliable H-G plot to be constructed and H and G parameters to be found. The first session 2014 Jan. 16 at phase angle 15.6 degrees showed an amplitude 0.10 magnitudes. Thirty additional sessions from 2014 Jan. 31 at phase angle 11.5 degrees pre-opposition to March 3 at minimum phase angle 2 degrees to May 4 at phase angle 18.0 degrees post-opposition all provide a good fit among sessions with full phase coverage for both a period of 21.812 ± 0.001 hours and the double period of 43.622 ± 0.001 hours. These data definitively ruled out all of the shorter periods. Unlike the lightcurves from the 2010, 2011, and 2012 oppositions, the usual bimodal behavior occurs, although with smaller amplitude only 0.08 ± 0.01 magnitudes and an unsymmetrical shape. We interpret the 0.10 magnitude amplitude 2014 Jan. 16 as due to the commonly occurring behavior among most asteroids of larger amplitudes at larger phase angles. Many of the sessions in 2014 April and May are of shorter time interval and do not cover a large enough section of the lightcurve to reveal any increase of amplitude which may have occurred with larger phase angle. They are valuable to extend the H-G plot to larger post-opposition phase angles but do not significantly improve the lightcurve.

Specifically for each year we present a separate period spectrum between 7 and 47 hours to cover all previously reported periods and also double the most likely period near 21.8 hours. Deep minima occur only near 21.8 hours and the double period of 43.6 hours, and all other reported periods are now ruled out. We also present for each of these three years new lightcurves based on a collection of all observations for each year and phased to both near 21.8 hours and 43.6 hours. To interpret the double period lightcurve we note the following. If 43.6 hours is twice the real period then segments of the lightcurve separated by phase 0.5 will be identical within errors of observation. This is noted for the available parts of all four 43.6 hour lightcurves. For the 2010 and 2011 lightcurves missing segments comprise less than 10% of the total lightcurve. For the 2012 lightcurve the sampling is less complete and the only available corresponding segments are those between phases 0.3-0.4 and 0.8-0.9, respectively. The 2014 lightcurve includes full phase coverage. All available evidence from all four years is therefore consistent with the hypothesis that 43.6 hours is the double period. An alternate interpretation that 43.6 hours is the real period requires a shape model highly symmetric over a 180 degree rotation which is extremely unlikely for a real asteroid.

The comparison stars for the sessions with clear and R band filter were calibrated to the R magnitude standard system, using the method described by Dymock and Miles (2009) and CMC-15 catalogue via VizieR Service (2014), while for the V band sessions the comparison stars were calibrated to the V magnitude standard system using the APASS catalogue. All the standardized clear and R band lightcurves were converted to the V band system adding the color index value V-R = 0.36 ± 0.03, obtained in the session of February 24, 2014 (Figure 14) and, for each lightcurve, the rotational effects, although small, was removed using Fourier fit model (Buchheim, 2010).

The absolute magnitude (H) and slope parameter (G) were found using the H-G calculator function of MPO Canopus. We have achieved H = 7.45 ± 0.01, G = 0.11 ± 0.02 (Figure 13). Both the color index and G value are compatible with a low albedo asteroid (Shevchenko and Lupishko, 1998). Note that our H value is quite different from H = 7.62, published on the JPL Small-Body Database Browser (JPL, 2014). The diameter is estimated to be D = 175 ± 33 km, assuming a geometric albedo pv = 0.06 ± 0.02 for C-type asteroid (Shevchenko and Lupishko, 1998) and using the formula by Pravec and Harris (2007). This value is consistent with other published values: 158 ± 3 km (IRAS), 168 ± 3 km (AKARI), 155 ± 5 km (WISE) and particularly close to 172 ± 7 km, obtained by occultations (Broughton, 2014).

The rotational lightcurve of 185 Eunike appears to be dominated by a hemispheric albedo dichotomy. This property is analogous to the hemispheric albedo dichotomy of 4 Vesta, as has been found from several independent investigations. Degewij et al. (1978) used polarimetry for the first verification that Vesta's monomodal 5.34 hour lightcurve is dominated by albedo. Drummond et al. (1988) used speckle interferometry to measure the hemispheric scale albedo variegations. Binzel et al. (1997) and Drummond et al. (1998) mapped these albedo variegations in greater detail with Hubble Space Telescope images and ground based adaptive optics images, respectively. The most detailed analysis of this 10% albedo variegation with global subkilometer scale Dawn spacecraft images has been published by Reddy et al. (2013).

Compared with the 570 x 570 x 460 kilometer triaxial dimensions of Vesta (Reddy et al. 2013), the diameter of 185 Eunike from WISE observations is only about 155 kilometers (Warner et al. 2014). This is, however, large enough that the Earth based techniques used for Vesta may be useful also for 185 Eunike. Polarimetry and speckle interferometry are hardly used nowadays, but adaptive optics imaging and narrow band spectroscopy extended over the full 21.8 hour rotational cycle should be highly productive. We recommend this procedure to all readers who may have access to the relevant equipment, especially at the 2016 September opposition. At this time Eunike will have geocentric distance 1.43 AU, nearly the minimum possible, and with a 155 kilometer diameter an angular size approximately 0.15 arcseconds.

Lightcurve Inversion

The not negligible number of lightcurves obtained so far at various phase angles and phase angle bisectors (table I), allow us to attempt the lightcurve inversion process. Figures 15, 16 show respectively PAB Longitude distribution and PAB Longitude/ Latitude distribution for the entire dense data set used. The lightcurve inversion process was performed using MPO LCInvert v.11.1.0.2. Software (Bdw Publishing).

All data were imported in *LCInvert* for analysis, binning them at time interval of 15 minutes. The “dark facet” weighting factor was

increased from 0.1 (default) to 0.8 to keep the dark facet area below 1% of total area, maybe due to the albedo variations. The number of iterations of processing was increased from 50 (default) to 100 for best convergence.

We have started the sidereal period search centered on the average of the synodic periods found in the years 2010, 2011, 2012 and 2014. The search process found a quite well isolated sidereal period of 21.80629277 h with lower chi-square value (Figure 17).

For pole search we have started using the "Medium" search option (312 fixed pole positions with 15° longitude-latitude steps) and the previously found sidereal period set to "float".

The data analysis does not show any isolated lowest chi-square values and additional sparse data from USNO Flagstaff does not bring any improvement, so we used only dense data. Therefore the found period/pole determination can not be considered very robust but only a preliminary solution.

The pole search found two cluster with similar lowest chi-square solution, centered around (λ = 135°, β = -30°) and (λ = 300°, β = 0°), within a radius of 30-40 degrees, see Figure 18 for log(chi-square) values distribution.

Refining the pole search again, using the "Fine" option (49 fixed pole steps with 10° longitude-latitude pairs) and the previous period/longitude/latitude set to "float", we found two best solutions at (λ = 136°, β = 4°), (λ = 314°, β = -18°) differing by 180° in longitude, with an averaged sidereal period Ps = 21.80634 ± 0.00012 h, obtained from the two previous solutions. The uncertainty in period has been evaluated as a rotational error of 30° over the total time-span of the observations.

Figures 19 and 20 show respectively the shape model (first solution) and the good fit agreement between the model (black line) and observed lightcurves (red points).

Acknowledgments

Author AM thanks the Tzec Maun Observatory (New Mexico Skies, Mayhill) for telescope time at which most of his data were obtained. The authors LF and FP thanks Dr. Josef Durech for the advice in the LCI analysis.

Author	Year	#LCs	PA°	PABL°	PABB°
Debehogne	1977	2	12	97	-25
Behrend	2005	2	9/10	168/166	5/9
Behrend	2010	11	10/15	200	22
Ruthroff	2010	7	10/13	200	22
Pilcher	2011	5	12/9	292	22/20
Ruthroff	2011	5	11/13	292	19/18
Hills	2012	8	16/14	61/63	-30
Pilcher	2014	27	15/18	162/163	0/9

Table I. Observational circumstances for 186 Eunike over six apparitions, a total of 67 lightcurves were used for lightcurve inversion analysis. Where: PA, PABL and PABB are respectively the phase angle, phase angle bisector longitude and latitude.

References

Bdw Publishing (2013), *http://www.minorplanetobserver.com/MPOSoftware/MPOLCInvert.htm*

Behrend, R. (2005, 2010). Observatoire de Geneve web site *http://obswww.unige.ch/~behrend/page_cou.html*

Binzel, R.P., Gaffey, M.J., Thomas, P.T., Zellner, B.H., Storrs, A.D., Wells, E.N. (1997). "Geologic mapping of Vesta from 1994 Hubble Space Telescope images." *Icarus* **128**, 95-103.

Broughton J., (2014). *http://www.asteroidoccultation.com/observations/Asteroid_Dimensions_from_Occultations.html#Table1*

Dymock, R., Miles, R. (2009). "A method for determining the V magnitude of asteroids from CCD images." *J. Br. Astron. Assoc.* **119**, 149-156.

Debehogne, H., Surdej, J., Surdej, A. (1978). "Photoelectric lightcurves of the minor planets 29 Amphitrite, 121 Hermione, and 185 Eunike." *Astron. Astrophys. Suppl. Ser.* **32**, 127-133.

Degewij, J., Tedesco, E.F., Zellner, B.H. (1979). "Albedo and color contrasts on asteroid surfaces." *Icarus* **40**, 364-374.

Drummond, J., Eckart, A., Hege, E.K. (1988). "Speckle interferometry of asteroids." *Icarus* **73**, 1-4.

Drummond, J.D., Fugate, R.Q., Christou, J.C. (1998). "Full adaptive optics images of Asteroids Ceres and Vesta rotational poles and triaxial ellipsoid dimensions." *Icarus* **132**, 80-99.

Hills, K. (2013). "Asteroid Lightcurve Analysis at Riverland Dingo Observatory (RDO): 185 Eunike, (17252) 2000 GJ127, and (152858) 1999 XN35." *Minor Planet Bull.* **40**, 89-90.

JPL (2014). *http://ssd.jpl.nasa.gov/sbdb.cgi*

Pilcher, F., Ruthroff, J.C. (2012). "Rotation Period Determination for 185 Eunike." *Minor Planet Bull.* **39**, 13.

Pravec, P. Harris, A.W. (2007). "Binary Asteroid Population 1. Angular Momentum Content." Icarus **158**, 106-145.

Reddy, V., and 12 co-authors (2013). "Comparing Dawn, Hubble Space Telescope, and ground-based interpretations of (4) Vesta." *Icarus* **226**, 1103-1114.

Ruthroff, J.C. (2010). "Lightcurve Analysis of Main Belt Asteroids 185 Eunike, 567 Eleutheria, and 2500 Alascattalo." *Minor Planet Bull.* **37**, 158-159.

Ruthroff, J.C. (2011). "Lightcurve Analysis of Eight Main-Belt Asteroids and a Revised Period for 185 Eunike." *Minor Planet Bull.* **38**, 86-88.

Shevchenko V.G., Lupishko D.F. (1998). "Optical properties of Asteroids from Photometric Data", *Solar System Research* **32**, 220-232.

VizieR (2014). *http://vizier.u-strasbg.fr/viz-bin/VizieR*

Warner, B.D., Harris, A.W., Pravec, P. (2014). "Asteroid Lightcurve Data File, March 1, 2014." *http://www.minorplanet.info/lightcurvedatabase.html.*

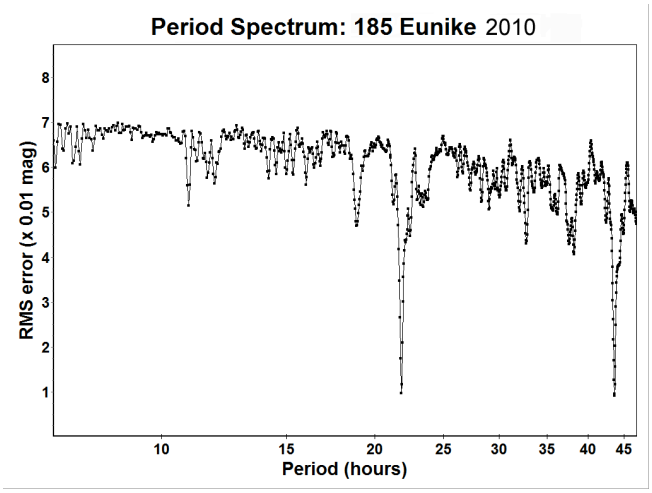

Figure 1. Period spectrum of year 2010 observations of 185 Eunike.

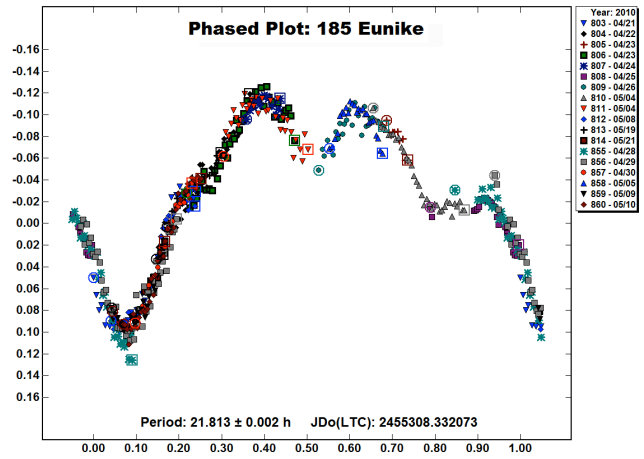

Figure 2. Year 2010 observations of 185 Eunike phased to a period 21.813 hours.

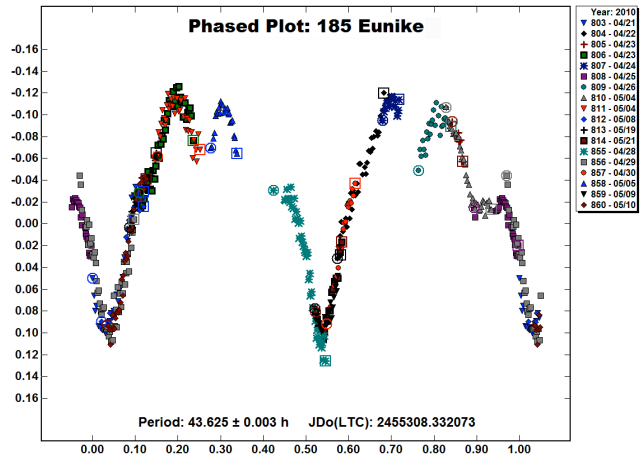

Figure 3. Year 2010 observations of 185 Eunike phased to the double period 43.625 hours.

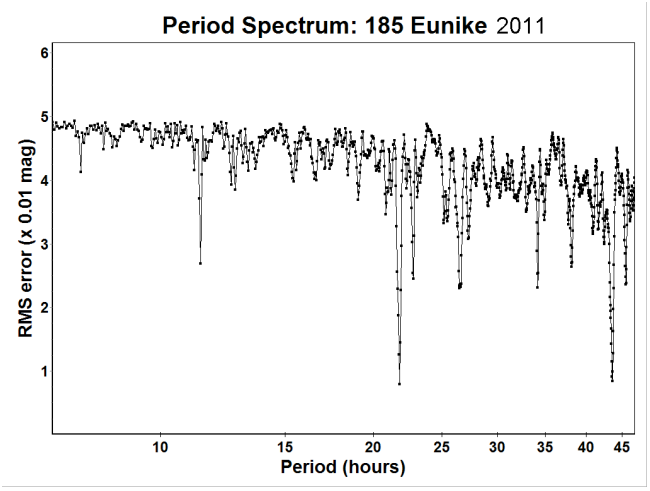

Figure 4. Period spectrum of year 2011 observations of 185 Eunike.

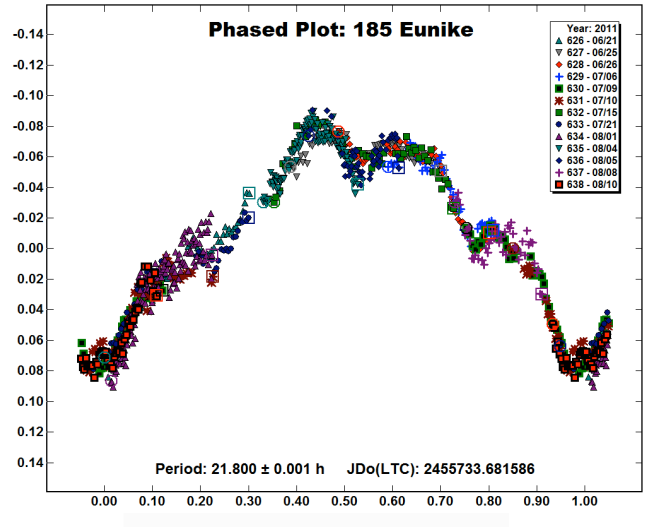

Figure 5. Year 2011 observations of 185 Eunike phased to a period 21.800 hours.

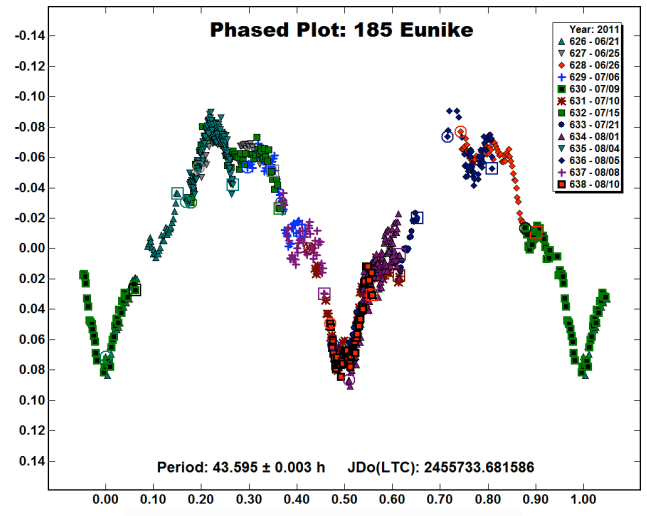

Figure 6. Year 2011 observations of 185 Eunike phased to the double period 43.595 hours.

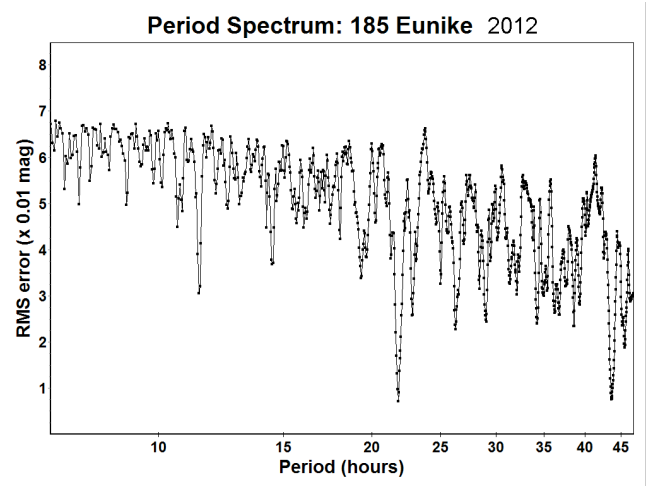

Figure 7. Period spectrum of year 2012 observations of 185 Eunike.

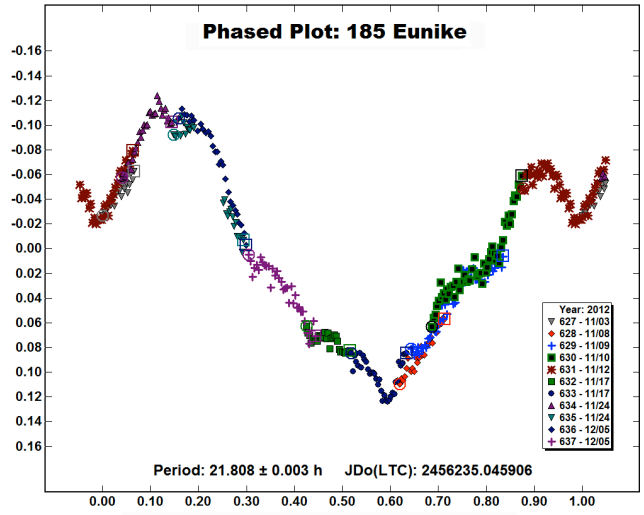

Figure 8. Year 2012 observations of 185 Eunike phased to a period 21.808 hours.

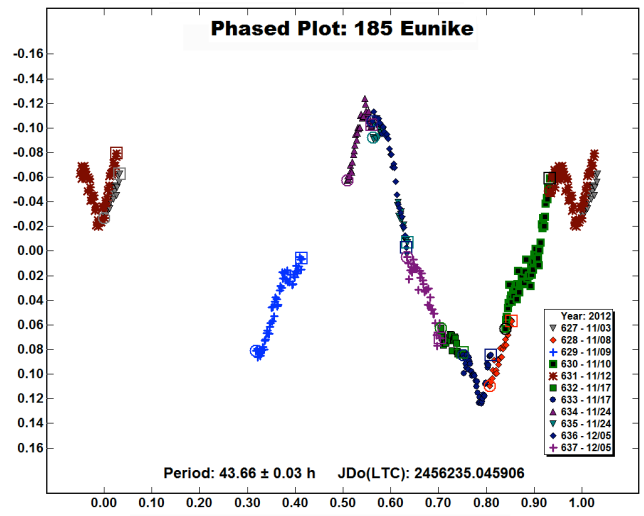

Figure 9. Year 2012 observations of 185 Eunike phased to the double period 43.66 hours.

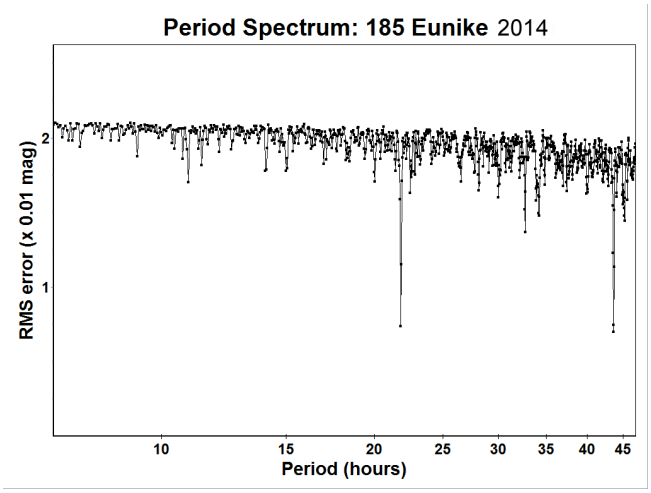

Figure 10. Period spectrum of year 2014 observations of 185 Eunike.

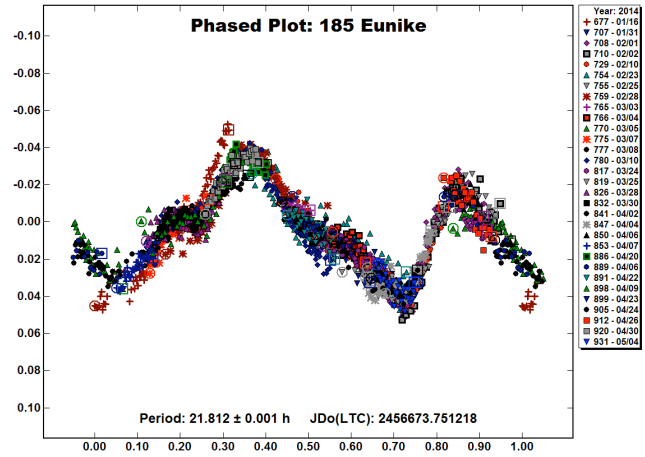

Figure 11. Year 2014 observations of 185 Eunike phased to a period 21.812 hours.

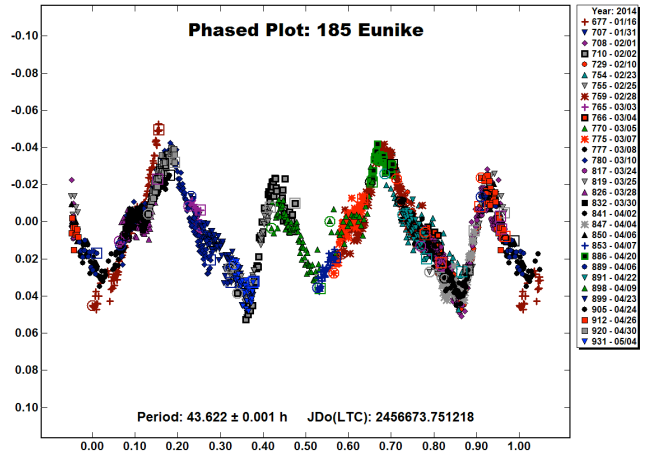

Figure 12. Year 2014 observations of 185 Eunike phased to the double period 43.622 hours.

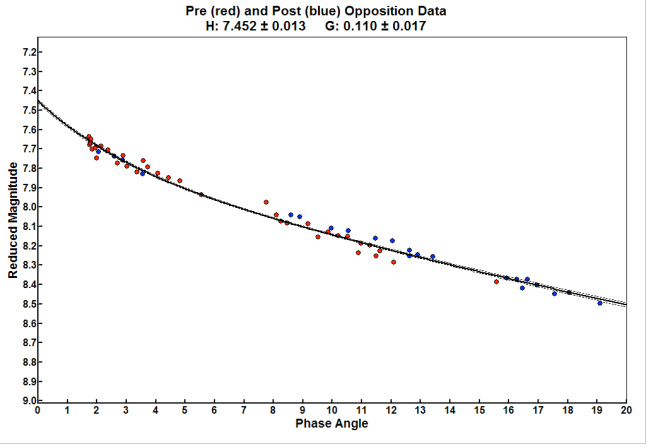

Figure 13. H-G plot of year 2014 observations of 185 Eunike converted to V magnitude system.

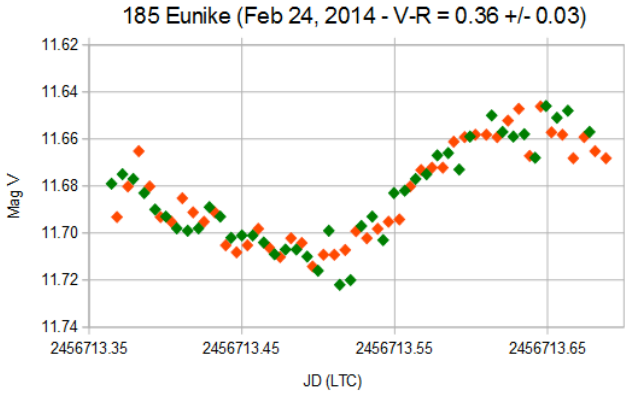

Figure 14. V and R lightcurve of 185 Eunike on 2014 Feb. 24.

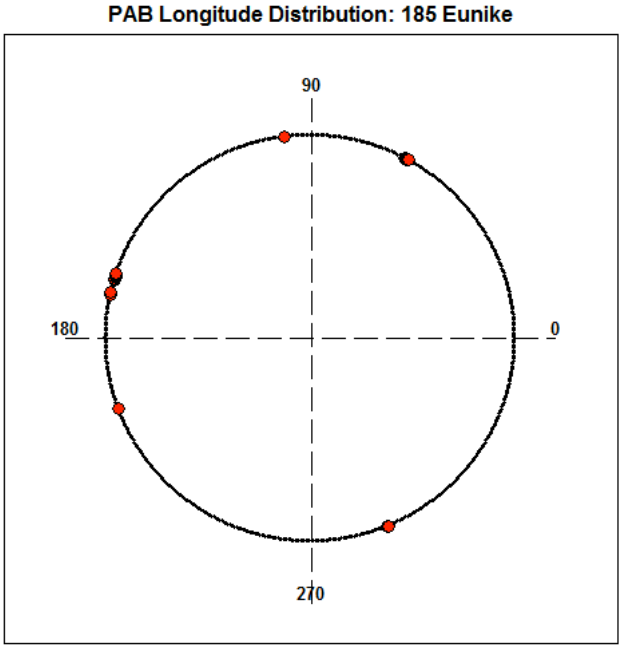

Figure 15. PAB Longitude distribution of the dense data used for lightcurve inversion model.

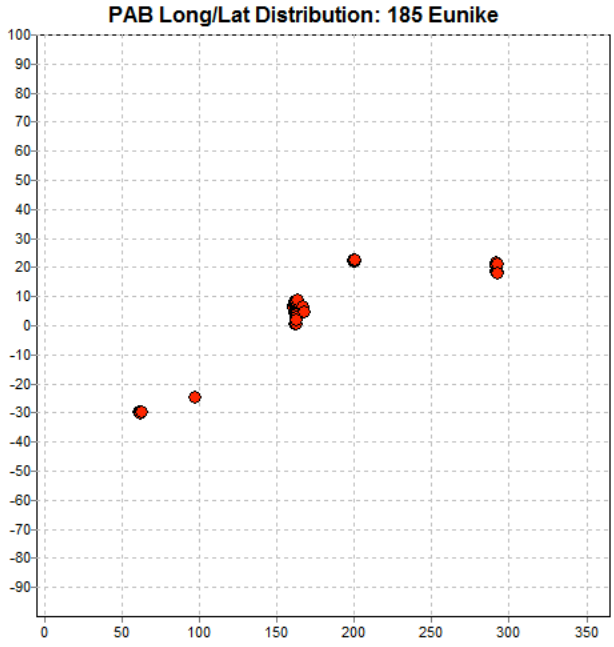

Figure 16. PAB Longitude and Latitude distribution of the dense data used for lightcurve inversion model.

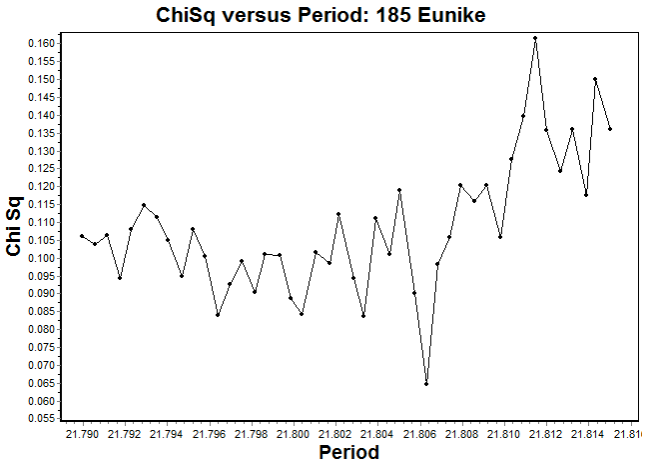

Figure 17. The period search plot from LCInvert shows a quite well isolated minimum at 21.80629277 h.

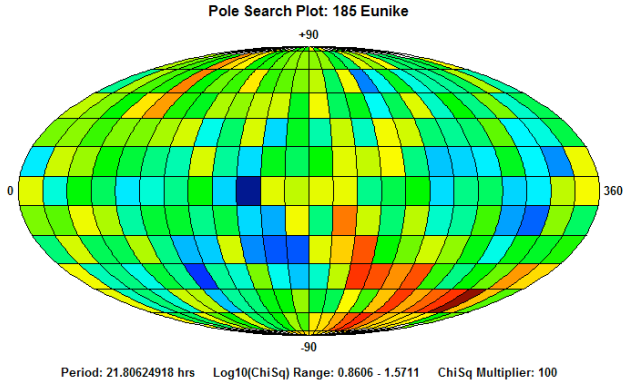

Figure 18. Pole Search Plot of log(ChiSq) values, where dark blue identify lower ChiSq values and Dark red underlying the worst solutions.

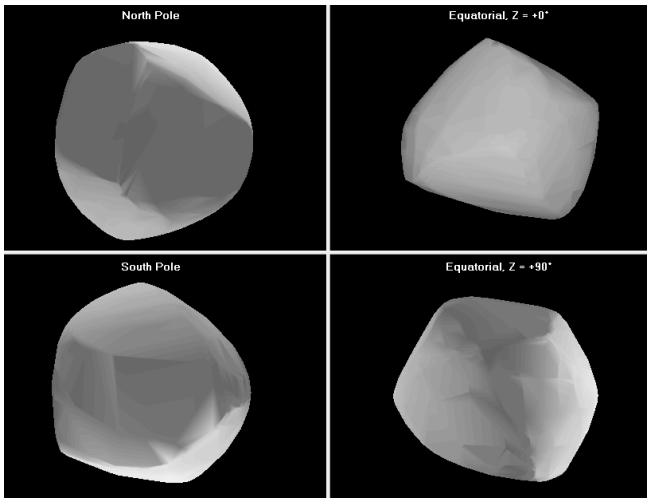

Figure 19. The shape model for 185 Eunike (λ = 136°, β = 4°).

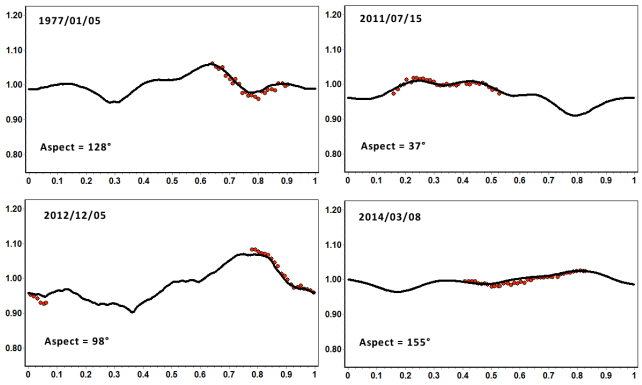

Figure 20. Comparison of model lightcurve (black line) versus a sample of four observed lightcurves (red points).